



**Triarylamine-Based Crosslinked Hole-Transporting Material
with a Ionic Dopant for High-Performance PEDOT:PSS-Free
Polymer Solar Cells**

Journal:	<i>Journal of Materials Chemistry C</i>
Manuscript ID:	TC-ART-03-2015-000714.R1
Article Type:	Paper
Date Submitted by the Author:	16-Apr-2015
Complete List of Authors:	Tsai, Che-En; National Chiao Tung University, Department of Applied Chemistry Liao, Ming-Hung; National Chiao Tung University, Department of Applied Chemistry Chen, Yung-Lung; National Chiao Tung University, Department of Applied Chemistry Cheng, Sheng-Wen; National Chiao Tung University, Department of Applied Chemistry Lai, Yu-Ying; National Chiao Tung University, Department of Applied Chemistry Cheng, Yen-Ju; National Chiao Tung University, Department of Applied Chemistry Hsu, Chain Shu; National Chiao Tung University,

ARTICLE

Triarylamine-Based Crosslinked Hole-Transporting Material with an Ionic Dopant for High-Performance PEDOT:PSS-Free Polymer Solar Cells

Cite this: DOI: 10.1039/x0xx00000x

Che-En Tsai, Ming-Hung Liao, Yung-Lung Chen, Sheng-Wen Cheng, Yu-Ying Lai, Yen-Ju Cheng* and Chain-Shu Hsu*

Received 00th January 2012,
Accepted 00th January 2012

DOI: 10.1039/x0xx00000x

www.rsc.org/

A triarylamine-based material DVTPD containing two styryl groups has been developed. Upon isothermal heating at 180 °C for 30 min, DVTPD can be thermally cross-linked to form a solvent-resistant layer to realize the fabrication of the solution-processed multilayer devices. The crosslinked DVTPD (denoted as X-DVTPD) layer possesses not only hole-collecting ability ($E_{\text{HOMO}} = -5.3$ eV) but also electron-blocking capability ($E_{\text{LUMO}} = -2.2$ eV). By incorporation of an ionic dopant, 4-isopropyl-4'-methyl-diphenyliodonium tetrakis(pentafluorophenylborate) (DPITPFB), into the X-DVTPD material (1:10 in wt%), a favourable morphology of the dopant/matrix layer was formed and the hole-mobility is significantly improved by three orders of magnitude compared to its non-doped state. This DPITPFB:X-DVTPD (1:10 in wt%) layer was employed as the hole-transporting layer to fabricate the polymer solar cell devices (PSCs). The E_{HOMO} of the polymer in the active layer relative to the E_{HOMO} of the X-DVTPD (-5.3 eV) governs the hole transportation highly associated with the device performance. The higher-lying E_{HOMO} (-5.0 eV) of P3HT causes a large energy barrier for the hole transportation at the interface, leading to an unsatisfactory efficiency. The E_{HOMO} level of the PTB7 copolymer (-5.15 eV) is closer to -5.3 eV. As a result, the PTB7-based device can achieve 80% of the efficiency obtained from the corresponding PEDOT:PSS-based device. Furthermore, PBDCPDTFBT copolymer has the same E_{HOMO} (-5.3 eV) with X-DVTPD. Consequently, PBDCPDTFBT-based device showed the comparable efficiency of 5.3% to the corresponding PEDOT:PSS-based device. More importantly, PNDDTDFBT having the lowest-lying E_{HOMO} of -5.4 eV leads to the superior performance with a high PCE of 6.64%, outperforming its reference PEDOT:PSS-based device. This simple and useful hole-transporting system integrating the crosslinking and doping strategies to replace PEDOT:PSS can be widely used in the solution-processed organic electronic devices.

Introduction

Polymeric solar cells (PSCs) are a promising alternative for clean and renewable energy due to their potential to be fabricated onto large area, light-weight and flexible substrates by solution processing at a lower cost.¹ PSCs consist of a bulk heterojunction (BHJ) active layer in which the p-type material and n-type material can form interpenetrating and bicontinuous charge pathways.² Currently, the power conversion efficiency (PCE) of the PSCs can reach higher than 8%.³ High transparent poly(3,4-ethylenedioxythiophene):polystyrenesulfonate (PEDOT:PSS) is the most widely used hole-conducting layer in the polymer light-emitting diodes (PLEDs) and PSCs due to the high conductivity and Ohmic contact with ITO.⁴ However, the acidic nature of PEDOT:PSS could chemically etch the ITO surface, resulting in the degradation of the device.⁵ Furthermore, using water-dissolved PEDOT:PSS inevitably increases water and oxygen content in the

devices, which is a major obstacle in the industry manufacture. Other disadvantages of PEDOT:PSS such as unstable morphology⁶, electrical inhomogeneity⁷ and electron-blocking inability⁸ were also documented. Therefore, searching for new organic materials to substitute the traditional PEDOT:PSS is desirable for both academic interest and industrial application.

Biphenyl diamine-based molecules such as TPD (*N,N'*-di-tolyl-*N,N'*-diphenyl-1,1'-biphenyl-4,4'-diamine) have been frequently used as the hole-transporting layers in organic light-emitting diodes owing to their good redox reversibility and electron-blocking ability.⁹ The TPD-based small molecules require sophisticated and time-consuming vacuum deposition to form the thin films which suffer unsatisfactory morphological stability as a result of the low glass transition temperatures.¹⁰ A more feasible method to make a TPD-based hole-transporting layer for PSCs is via a solution-processing technique. However, a problematic challenge in fabricating a multilayer device by spin coating is that the coated

layer will be partially re-dissolved by the solvent used in the following processing step. To alleviate this problem, many strategies such as self-assembled layer¹¹, orthogonal solvents¹² and chemical crosslinking¹³ have been presented. We have recently reported a crosslinkable TPD-based HTM *N,N'*-bis(tolyl)-*N,N'*-bis(vinylphenyl)-1,1'-biphenyl-4,4'-diamine (DVTPD) (**Figure 1**).¹⁴ The two styryl groups in DVTPD can undergo thermal-induced crosslinking without initiator¹⁵ upon heating to form a robust and solvent-resistant layer, thus avoiding the interfacial mixing. Although these materials can be technically inserted as an electron-blocking layer in the multilayer light-emitting diodes, integration with a PEDOT:PSS layer remains necessary to achieve the high-performance devices due to the fact that the limited effective conjugation length and amorphous nature of TPD-based materials exhibit only moderate hole mobilities.^{14, 16} Similarly, the attempt to completely replace the water-based PEDOT:PSS with a single crosslinked HTM layer for PSCs has not been successful so far.

Electrical doping in organic semiconductors has been demonstrated as a powerful strategy to improve the charge mobility and reduce the injection barrier.¹⁷ It is envisaged that the TPD derivatives incorporated with a p-dopant will greatly improve the mobility in comparison with the non-doped state, while maintaining its electron-blocking ability because of the intrinsic high-lying lowest unoccupied molecular orbital (LUMO) level. Moreover, by simply adjusting the dopant/matrix ratio, the charge transporting properties of HTMs can be fine-tuned and controlled. Surprisingly, the combination of a crosslinkable HTM with a p-dopant for polymer solar cells is only sporadically reported.¹⁸ Ionic iodonium-based materials have been extensively synthesized and investigated.¹⁹ In this research, 4-isopropyl-4'-methylphenyliodonium tetrakis(penta-fluorophenylborate) (DPITPFB) is selected as an ionic p-dopant (**Figure 1**). The hole-mobility of the crosslinked DVTPD (X-DVTPD) layer increases dramatically after p-doping of DPITPFB (*ca.* 9 % in wt). With the higher mobility and better hole-collection ability, the solar cell devices using a X-DVTPD matrix p-doped with the DPITPFB exhibited significantly enhanced V_{oc} , J_{sc} , and FF parameters leading to the power conversion efficiencies comparable to those of the corresponding PEDOT:PSS-based devices. The detailed investigation and application for PSCs will be discussed.

Results and Discussion

The solvent-resistance after thermal crosslinking

Differential scanning calorimetry (DSC) was employed to determine the cross-linking temperature of DVTPDMe (**Figure 2**). The exothermal peaks from 120 °C to 147 °C were observed at the first scan, which is indicative of thermal polymerization of the styryl groups, while there is no peak during the second DSC scan. Solvent resistance of the crosslinked DVTPD matrix was evaluated by monitoring the UV-visible spectra of the thin films before and after rinsing with chlorobenzene which is a good solvent for DVTPD. (**Figure 3**) The crosslinking degree (CD) of the X-DVTPD to quantify the solvent resistance is defined as the absorbance at 355 nm before rinsing versus after rinsing (after λ_{355} /before λ_{355}). The isothermal heating at 170 °C for

15 min only led to a CD of 70%. Increase of the heating temperature to 180 °C improves the CD to 80%. Eventually, the isothermal heating at 180 °C for 30 min resulted in high solvent resistance with a CD up to 97%. In contrast, the pristine thin film without thermal-induced crosslinking showed almost no absorbance after rinsing, meaning that the uncrosslinked film does not have any solvent resistance. Based on the results, the isothermal heating at 180 °C for 30 min is selected as the crosslinking condition for the device fabrication.

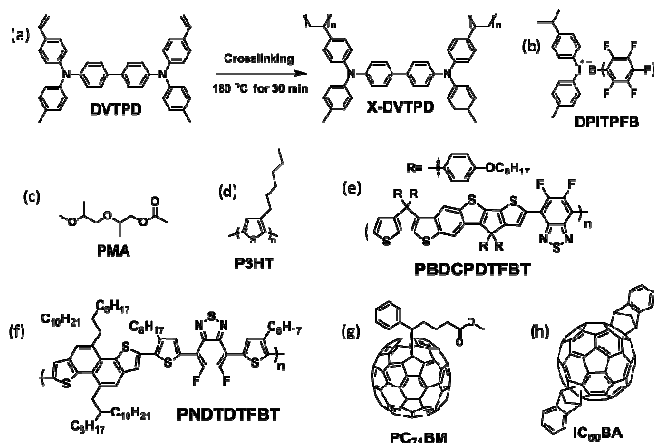


Figure 1. The chemical structures of the materials used in this research. (a) DVTPD and X-DVTPD; (b) DPITPFB; (c) non-halogen solvent, PMA; (d) P3HT; (e) PBDCPDTFBT polymer; (f) PNDDTTFBT polymer; (g) PC₇₁BM; (h) IC₆₀BA.

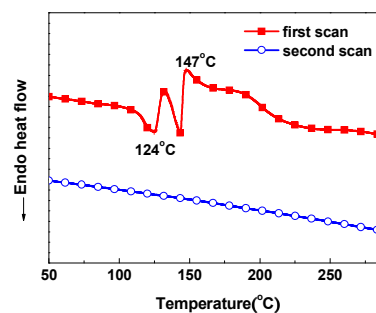


Figure 2. The first and second DSC scans of DVTPDMe with a ramping rate of 10 °C/min.

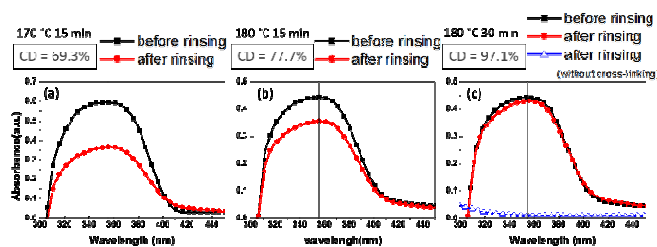


Figure 3. UV-visible spectra of the thin films before (black curves) and after rinsing (red curves) with chlorobenzene. (a) 170 °C thermal

heating for 15 min, (b) 180 °C thermal heating for 15 min, (c) 180 °C thermal heating for 30 min.

Mobility improvement by chemical doping

Chemical doping has been demonstrated as a useful strategy to improve the charge mobility of semiconductors. The mobility of the DPITPFB-doped X-DVTPD layer was measured by the hole-only devices fabricated with the configuration of ITO/DPITPFB:X-DVTPD/Au using space-charge-limited-current (SCLC) theory.²⁰ The DVTPD solution was first spin-casted on the ITO and heated at 180 °C for 30 min to form the X-DVTPD. In order to investigate concentration effect of the dopant on the mobility, the DPITPFB, dissolved in an environmentally friendly non-halogen solvent, propylene glycol monomethyl ether acetate (PMA, see Figure 1), was dropped on the surface of the X-DVTPD. After waiting for different time of 0, 15, 30 and 45 second for penetration, the substrates were spun at 6000 rpm and washed by PMA to remove the DPITPFB residue. Encouragingly, we found that the mobility is proportional to the dopant penetration time (**Figure 4(a)**), which confirms that the DPITPFB can serve as a chemical dopant to increase the hole-mobility of X-DVTPD. After demonstrating the effect of DPITPFB, we directly added DPITPFB into the DVTPD solution with different weight ratio (DPITPFB:DVTPD = 1:12, 1:10, 1:5, 1:3 in wt%) for the fabrication of the hole-only devices (ITO/(DPITPFB:X-DVTPD/DVTPD)/Au) in which an additional neutral DVTPD layer was used as an electron-blocking layer. It should be noted that the incorporation of the DPITPFB into the X-DVTPD does not affect its crosslinking condition. The undoped X-DVTPD layer exhibited a mobility of $1.3 \times 10^{-6} \text{ cm}^2 \text{ V}^{-1} \text{ s}^{-1}$. After doping with DPITPFB, the mobility dramatically increased by more than three orders of magnitude. When the content of the DPITPFB dopant increased in the matrix (1:12, 1:10, 1:5 in wt%), the mobility enhanced slightly to 5.7×10^{-3} , 6.8×10^{-3} , and $9.1 \times 10^{-3} \text{ cm}^2 \text{ V}^{-1} \text{ s}^{-1}$, respectively, (**Figure 4(b)**) with the concomitant reduction of the turn-on voltages. It is therefore envisaged that this dopant/matrix system could replace the PEDOT:PSS to function as a hole-transporting layer for the PSC applications.

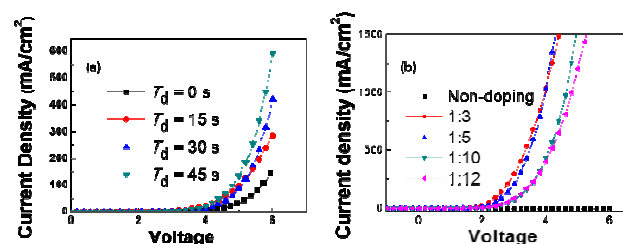


Figure 4. *J-V* curves of the hole-only devices. (a) The device configuration: ITO/DPITPFB:X-DVTPD ($T_d = 0, 15, 30$ and 45 s penetration time of the dopant solution)/Au. (b) The device configuration: ITO/DPITPFB:X-DVTPD (1:12, 1:10, 1:5, 1:3 wt%)/DVTPD/Au.

Table 1. Hole-mobility of the dopant:matrix thin films measured by the hole-only devices.

Weight ratios (wt%)	Mobility ($\text{cm}^2 \text{ V}^{-1} \text{ s}^{-1}$)
DVTPD	1.3×10^{-6}
DPITPFB:X-DVTPD = 1:12	5.7×10^{-3}
DPITPFB:X-DVTPD = 1:10	6.8×10^{-3}
DPITPFB:X-DVTPD = 1:5	9.1×10^{-3}
DPITPFB:X-DVTPD = 1:3	7.7×10^{-3}

Morphology of the dopant/matrix thin films

The blending ratio between the DVTPD and DPITPFB in the PMA solution will significantly influence the nanostructured morphology of the thin film which in turn plays an important role in determining the hole-mobility and electron-blocking ability. The DPITPFB is an ionic small molecule that tends to aggregate in the high concentration. Consequently, too much DPITPFB dopant in the X-DVTPD matrix will detrimentally cause the formation of morphological defects due to the phase separation. Atomic force microscope (AFM) was used to investigate the surface morphology of the thin films with different DPITPFB:X-DVTPD weight ratios (**Figure 5**). The non-doped X-DVTPD film exhibited a smooth RMS roughness of 1.30 nm. However, the obvious particles were formed in the thin film of 1:3 ratio, and the roughness dramatically increased to 14.7 nm. The unfavourable morphology will lead to the serious dark current and decrease the fill factor and J_{sc} .²¹ When the content of DPITPFB was reduced to 1:5, the roughness of the thin films decreased to 1.9 nm. The thin film of 1:10 ratio showed a very homogeneous morphology with a roughness of 1.53 nm.

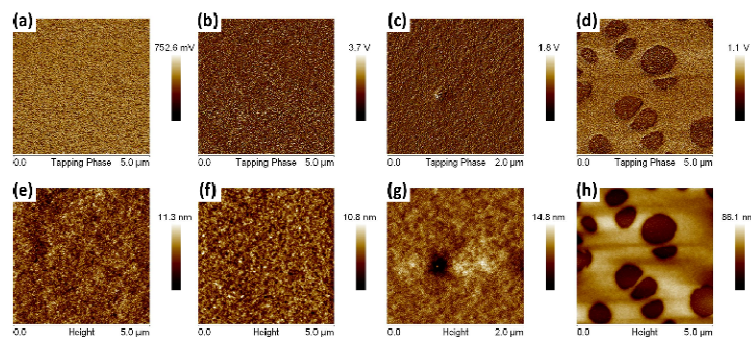


Figure 5. The AFM images of the DPITPFB:X-DVTPD blending thin films. Tapping phase of the X-DVTPD films (a) without doping, doped with DPITPFB (b) 1:10, (c) 1:5, (d) 1:3 wt%, respectively. Topography of the X-DVTPD films (e) without doping, doped with DPITPFB (f) 1:10, (g) 1:5, (h) 1:3 in wt%, respectively. The RMS roughness is 1.59 nm, 1.53 nm, 1.90 nm, and 14.7 nm, respectively.

Covering ability of the dopant/matrix thin film

During the fabrication of the device, it is inevitable that some dust or particles in the atmosphere will deposit on the ITO surface. Deposition of the subsequent hole-transporting layer could generate the disconnected defects near the particles. Therefore, the ability of the hole-transporting layer to fully cover the shape of the particles is an important criterion to avoid severe defects in the solution-

processable multilayer devices. To investigate the covering ability of the dopant/matrix system, we first intentionally dispersed silicon balls with diameter of 2 μm on the ITO substrate. The DPITPFB:DVTPD blending solution was then spin-cast and crosslinked on top of the surface of the ITO. Scanning electron microscopy (SEM) was used to observe the cross-section of the thin film. **Figure 6** shows that the edges of the silicon balls can be fully filled with the hole-transporting materials, indicating that the DPITPFB:X-DVTPD layer can thoroughly cover the particles to minimize the detrimental effects.

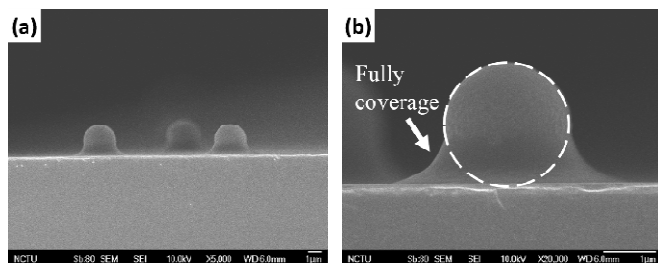


Figure 6. (a) The SEM image of the cross-section of the thin film. The silicon balls (2 μm of diameter) were first cast on the ITO surface followed by the formation of the DPITPFB:X-DVTPD thin film (1:10 in wt%). (b) The image magnified by 4 times.

Device characteristics and performances

After demonstrating the capability of the DPITPFB-doped X-DVTPD layer to replace the water-based PEDOT:PSS, we incorporated this dopant/matrix system as the hole-conducting layer into the conventional multilayer solar cells. To test its widespread capability, three donor-acceptor copolymers PTB7²², PBDCPDTFBT²³ and PNDTDTFBT blended with PC₇₁BM as well as P3HT blended with ICBA²⁴ were chosen as the photoactive materials for investigation (see Figure 1). The parameters and the J - V curves are shown in **Table 2** and **Figure 7(a)**. The crosslinking feature of the DVTPD to overcome the interlayer erosion allows us to fabricate the multilayer device via the spin-coating method. The standard device based on the ITO/PEDOT:PSS/PBDCPDTFBT:PC₇₁BM/Ca/Al exhibited a PCE of 5.31% with a J_{sc} of -11.80 mA/cm^2 , a V_{oc} of 0.82 V, a FF of 54.82%. By replacing the PEDOT:PSS with the non-doped X-DVTPD, the efficiency decreased dramatically to 1.07%, indicating the insufficient hole-mobility of the non-doped X-DVTPD layer. In contrast, when DPITPFB was doped into the X-DVTPD (1:10 in wt%) layer, the efficiency significantly enhanced to 5.30% which is already comparable to the PEDOT:PSS-based device. Note that the J_{sc} of 12.96 mA/cm^2 is even higher than of the PEDOT:PSS-based device (11.80 mA/cm^2). Nevertheless, further increasing the content of DPITPFB to 1:5 and 1:3 adversely deteriorated the efficiency to 4.55% and 1.50%, respectively, which is ascribed to the unfavourable morphologies associated with the aggregation of DPITPFB in the high concentration. Moreover, the optimal ratio of the DPITPFB:DVTPD (1:10 in wt%) is also adoptable to the PTB7:PC₇₁BM-based and PNDTDTFBT:PC₇₁BM-based devices. The standard device of ITO/PEDOT:PSS/PNDTDTFBT:PC₇₁BM/Ca/Al delivered a J_{sc} of

-10.77 mA/cm^2 and a PCE of 6.54%, while the counterpart device using the DPITPFB:X-DVTPD layer to replace PEDOT:PSS achieved an even higher J_{sc} of 11.69 mA/cm^2 and PCE of 6.64%. The EQE spectra of the two PNDTDTFBT:PC₇₁BM-based devices are shown in **Figure 7(b)**. On the other hand, the PTB7:PC₇₁BM-based device using PEDOT:PSS exhibited a PCE of 5.03%, while the corresponding device using the DPITPFB:X-DVTPD layer showed slightly decrease PCE of 4.46%. However, when the DPITPFB:X-DVTPD layer was applied to the P3HT:ICBA system, the efficiency of the device greatly decreased to 1.92%, which is much inferior to the PEDOT:PSS-based device with a PCE of 4.77%. Based on the analysis of the results, we observed that the variations of the device performance are highly dependent on the HOMO energy level (E_{HOMO}) of the p-type polymers. The energy diagrams of the polymers and X-DVTPD are illustrated in the **Figure 8a**, while **Figure 8b** shows the efficiency of the DPITPFB:X-DVTPD-based devices relative to the corresponding PEDOT:PSS-based devices as a function of the HOMO of the used polymer. The E_{HOMO} for P3HT, PTB7, PBDCPDTFBT and PNDTDTFBT are estimated to be -5.0 , -5.15 , -5.3 , and -5.4 eV , respectively. The E_{HOMO} of the X-DVTPD is *ca.* -5.3 eV . The energy offset between the E_{HOMO} of the two adjacent layers play an important role in determining the hole-transportation at the interfaces. The E_{HOMO} of P3HT (-5.0 eV) is much higher-lying than the X-DVTPD (-5.30 eV). The unmatched energy alignment between the two layers makes the hole extraction from the active layer to the HTL more difficult due to the large energy barrier (0.3 eV difference), leading to the much decreased J_{sc} (from -8.62 to -7.56) and FF (from 69.2 to 32.4%) compared to the standard PEDOT:PSS-based device. When the PTB7 copolymer ($E_{\text{HOMO}} = -5.15 \text{ eV}$) was employed, the DPITPFB:X-DVTPD layer became more effective to transport holes owing to the reduced energy offset (0.15 eV). Therefore, the device produced about the 85% of efficiency obtained from the corresponding PEDOT:PSS-based device. The PBDCPDTFBT copolymer has an identical E_{HOMO} of -5.3 eV with the X-DVTPD. Without the energy barrier at the interface, the PBDCPDTFBT-based device exhibited as good efficiency (5.3%) as the PEDOT:PSS-based device. More interestingly, the E_{HOMO} of PNDTDTFBT (-5.4 eV) is even lower than that of the X-DVTPD, which provides a downhill charge transportation pathway. As a result, the PNDTDTFBT-based device using the DPITPFB:X-DVTPD layer delivered the superior performance to the corresponding PEDOT:PSS-based device. These findings suggest that the DPITPFB:X-DVTPD system is specifically suitable and applicable for the low-band-gap polymers with E_{HOMO} lower than -5.3 eV . Fortunately, the current successful p-type polymers require much lower-lying E_{HOMO} which is an important criterion to reach the high V_{oc} for better performance. This distinct HOMO and V_{oc} relationship was also observed in our device characteristics showing that the PNDTDTFBT-based device has the highest V_{oc} of 0.84 V ($E_{\text{HOMO}} = -5.4 \text{ eV}$), followed by the PBDCPDTFBT-based device with the V_{oc} of 0.8 V ($E_{\text{HOMO}} = -5.3 \text{ eV}$), and PTB7-based device with the V_{oc} of 0.7 V ($E_{\text{HOMO}} = -5.15 \text{ eV}$). It should also be emphasized that the E_{HOMO} of the crosslinkable

host material can be tunable through molecular engineering in order to match the energy alignment of the different polymer materials.

Table 2 Fabrication conditions and device characteristics

polymers	HTL	V_{OC} (mA/cm ²)	J_{SC} (V)	PCE (%)	FF (%)
PBDCPDTFBT:PC ₇₁ BM (1:1.2 in wt%)	Withot HTL	0.50	-10.72	2.32	43.3
	PEDOT:PSS	0.82	-11.80	5.31 (5.21) ^a	54.9
	X-DVTPD	0.38	-8.17	1.07	34.6
	DPITPFB:X-DVTPD (1:10 in wt%)	0.80	-12.96	5.30 (5.14) ^a	51.1
	DPITPFB:X- DVTPD (1:5 in wt%)	0.80	-11.13	4.55	51.0
	DPITPFB:X- DVTPD (1:3 in wt%)	0.72	-5.01	1.50	41.7
PTB7:PC ₇₁ BM (1:1.5 in wt%)	PEDOT:PSS	0.74	-11.04	5.03	61.5
	DPITPFB:X-DVTPD (1:10 in wt%)	0.70	-11.11	4.46	57.4
PNDDTDFBT:PC ₇₁ BM (1:3 in wt%)	PEDOT:PSS	0.86	-10.77	6.54 (6.37) ^a	70.6
	DPITPFB:X-DVTPD (1:10 in wt%)	0.84	-11.69	6.64 (6.55) ^a	67.6
P3HT:ICBA (1:1 in wt%)	PEDOT:PSS	0.80	-8.62	4.77	69.2
	DPITPFB:X-DVTPD (1:10 in wt%)	0.78	-7.56	1.92	32.4

^a Average efficiency values over 10 devices.

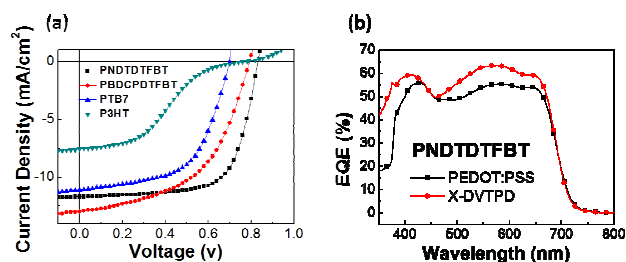


Figure 7. (a) J - V curves of ITO/DPITPFB:X-DVTPD/polymer:PC₇₁BM/Ca/Al device; polymer = PNDDTDFBT, PBDCPDTFBT, PTB7 and P3HT; (b) EQEs of ITO/DPITPFB:X-DVTPD/PNDDTDFBT:PC₇₁BM/Ca/Al and ITO/PEDOT:PSS/PNDDTDFBT:PC₇₁BM/Ca/Al devices.

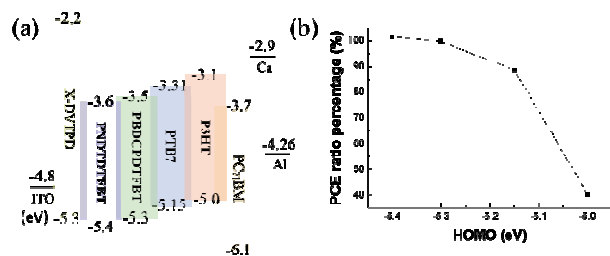


Figure 8. (a) The energy diagram of the multilayer PSC devices (X-DVTPD), (b) the device efficiencies of the DPITPFB:X-DVTPD-based device relative to the corresponding PEDOT:PSS-based device as a function of the HOMO energy level of the used polymer.

Conclusions

In conclusion, we have developed a styryl-functionalized triarylamine-based DVTPD material which can be thermally crosslinked at 180 °C for 30 min to form a solvent-resistant thin film with the good coverage ability for the fabrication of multilayer solar cells. The hole mobility of the crosslinked DVTPD can be significantly enhanced by three orders of magnitude through

incorporating an ionic DPITPFB dopant. The relative weight ratio between the DPITPFB and DVTPD was optimized to be 1:10 to achieve the good charge mobility and favourable morphology. The DPITPFB:X-DVTPD hole-transporting layer, processed by a non-halogen PMA solvent, was used to fabricate a series of devices incorporating p-type copolymers PTB7, PBDCPDTFBT, PNDDTDFBT and P3HT with different E_{HOMO} levels. The corresponding PEDOT:PSS-based devices were fabricated for comparison. It is found that the device performance is highly dependent on the energy offset between the E_{HOMO} of the X-DVTPD (-5.3 eV) and the E_{HOMO} of the polymer used in the active layer. The P3HT:ICBA-based device with the E_{HOMO} (-5.0 eV) of P3HT upwardly deviating from -5.3 eV showed the inferior device performance due to the high energy barrier for the charge transportation at the interface. With the E_{HOMO} level of PTB7 being closer to -5.3 eV, the PTB7-based device showed much improved device efficiency. Because the E_{HOMO} of PBDCPDTFBT is also at -5.3 eV, the BDCPDTFBT-based device exhibited an identical efficiency of 5.3% compared to the corresponding PEDOT:PSS-based device. More importantly, PNDDTDFBT having the lowest-lying E_{HOMO} of -5.4 eV exhibited the superior performance with a high PCE of 6.64%, outperforming the corresponding PEDOT:PSS-based device. In this research, we have successfully developed a simple and useful dopant/matrix strategy to achieve the high-performance PEDOT:PSS-free polymer solar cells.

Experimental Section

For the devices with a PEDOT:PSS (Baytron PVP Al4083) layer, a filtered (at 0.45 μ m) solution of PEDOT:PSS was spun-cast onto pre-cleaned ITO substrate (thickness is around 30 nm), and baked at 150 °C for 10 min in the glovebox. For the devices with a DPITPFB:X-DVTPD layer, the DVTPD was dissolved in PMA with a concentration of 10 mg/mL, and DPITPFB was added with the weight ratio needed (3:1, 5:1, 10:1, 12:1 in wt%). The filtered solution (at 0.45 μ m) was spin-cast onto pre-cleaned ITO substrate

(thickness is around 30 nm), and baked at 180 °C for 30 min for cross-linking in the glovebox. After cross-linking step, the device was kept in the glovebox for one day. The photoactive layer was deposited by spin-coating the filtered *o*-dichlorobenzene solution of the polymer:PC₇₁BM on DPITPFB:X-DVTPD layer, or PEDOT:PSS, or bare ITO in the glovebox. Then, the devices were covered with shadow masks to define the active area (0.04 mm²) and transferred into the thermal evaporator. The electrode consisting of calcium (35 nm) and aluminum (150 nm) was thermally evaporated on the active layer sequentially. PTB7 was purchased from Lumtec, the PC₇₁BM was purchased from UR. PTB7 was dissolved in chlorobenzene with concentration of 10 mg/mL (PTB7:PC₇₁BM weight ratio is 1:1.5), and 3 v% diiodooctane. PBDCPDTFBT was dissolved in *o*-dichlorobenzene with concentration of 6 mg/mL (PBDCPDTFBT:PC₇₁BM weight ratio is 1:3). PNDTDTFBT was dissolved in *o*-dichlorobenzene with concentration of 10 mg/mL (PNDTDTFBT:PC₇₁BM weight ratio is 1:1.2). P3HT and ICBA were both purchased from Lumtec. P3HT was dissolved in *o*-dichlorobenzene with concentration of 1.7 w% (P3HT:PC₆₁BM weight ratio is 1:1). For hole-only device fabrication, the configuration of device was ITO/doped X-DVTPD/neutral DVTPD/Au. The hole mobilities were calculated according to space-charge-limited-current theory (SCLC). The *J*-*V* curves were fitted according to the following equation: $J = (9/8) \epsilon \mu (V^2/L^3)$ where ϵ is the permittivity of the blend film, μ the hole mobility, and *L* the film thickness. All the devices were measured in air conditions using a Keithley 2400 SMU source measurement unit and the Oriel Xenon lamp (450 W) with an AM1.5 filter as the solar simulator. The light intensity was calibrated by a standardized reference silicon solar cell to 100 mW/cm².

Acknowledgements

We thank the Ministry of Science and Technology, the Ministry of Education, and the Center for Interdisciplinary Science (CIS) of the National Chiao Tung University, Taiwan, for financial support. We thank the National Center of High-Performance Computing (NCHC) in Taiwan for computer time and facilities. Y.J.C. acknowledges the support from the Golden-Jade fellowship of the Kenda Foundation, Taiwan.

National Chiao Tung University, Department of Applied Chemistry, 1001 University Road, Hsin-Chu, 30010, Taiwan

Email: yicheng@mail.nctu.edu.tw, and cshsu@mail.nctu.edu.tw

Notes and references

- (a) Y.-J. Cheng, S.-H. Yang and C.-S. Hsu, *Chem. Rev.*, 2009, **109**, 5868-5923. (b) Z. He, C. Zhong, S. Su, M. Xu, H. Wu and Y. Cao, *Nat. Photon.*, 2013, **6**, 591-595. (c) W. Li, A. Furlan, K. H. Hendriks, M. M. Wienk and R. A. Janssen, *J. Am. Chem. Soc.*, 2013, **135**, 5529-5532. (d) J.-S. Wu, S.-W. Sheng, Y.-J. Cheng, C.-S. Hsu, *Chem. Soc. Rev.*, 2015, **44**, 1113-1154.
- (a) G. Yu, J. Gao, J. C. Hummelen, F. Wudl and A. J. Heeger, *Science*, 1995, **270**, 1789-1791. (b) W. Ma, C. Yang, X. Gong, K. Lee and A. J. Heeger, *Adv. Funct. Mater.*, 2005, **15**, 1617-1622. (c) G. Li, V. Shrotriya, J. Huang, Y. Yao, T. Moriarty, K. Emery and Y. Yang, *Nat. Mater.*, 2005, **4**, 864-868. (d) S. H. Park, A. Roy, S. Beaupr e, S. Cho, N. Coates, J. S. Moon, D. Moses, M. Leclerc, K. Lee and A. J. Heeger, *Nat. Photon.*, 2009, **3**, 297-302.
- (a) J. You, L. Dou, K. Yoshimura, T. Kato, K. Ohya, T. Moriarty, K. Emery, C. C. Chen, J. Gao, G. Li and Y. Yang, *Nat. Commun.*, 2013, **4**, 1446-1455. (b) T. Yang, M. Wang, C. Duan, X. Hu, L. Huang, J. Peng, F. Huang and X. Gong, *Energy Environ. Sci.*, 2012, **5**, 8208-8214. (c) C. E. Small, S. Chen, J. Subbiah, C. M. Amb, S. W. Tsang, T. H. Lai, J. R. Reynolds and F. So, *Nat. Photonics*, 2012, **6**, 115-120. (d) Z. C. He, C. M. Zhong, X. Huang, W. Y. Wong, H. B. Wu, L. W. Chen, S. J. Su and Y. Cao, *Adv. Mater.*, 2011, **23**, 4636-4643. (e) R. F. Service, *Science*, 2011, **332**, 293-293. (f) L. Dou, W.-H. Chang, J. Gao, C.-C. Chen, J. You and Y. Yang, *Adv. Mater.*, 2013, **25**, 825-831. (g) S. M. Yoon, S. J. Lou, S. Loser, J. Smith, L. X. Chen, A. Facchetti and T. Marks, *Nano Lett.*, 2012, **12**, 6315-6321. (h) C. Cabanetos, A. E. Labban, J. A. Bartelt, J. D. Douglas, W. R. Mateker, J. M. J. Fr chet, M. D. McGehee and P. M. Beaujuge, *J. Am. Chem. Soc.*, 2013, **135**, 4656-4659. (i) Z. He, C. Zhong, S. Su, M. Xu, H. Wu and Y. Cao, *Nat. Photonics*, 2012, **6**, 591-595.
- (a) T. M. Brown, J. S. Kim, R. H. Friend, F. Cacialli, R. Daik and W. J. Feast, *Appl. Phys. Lett.*, 1999, **75**, 1679-1681. (b) R. Po, C. Carbonera, A. Bernardi and N. Camaioni, *Energy Environ. Sci.*, 2011, **4**, 285-310. (c) F. L. E. J. X. Crispin, A. Crispin, P. C. M. Grim, P. Andersson, A. Volodin, C. van Haesendonck, M. Van der Auweraer, W. R. Salaneck, and M. Berggren, *Chem. Mater.*, 2006, **18**, 4354-4360. (d) W. Hong, Y. Xu, G. Lu, C. Li and G. Shi, *Electrochem. Commun.*, 2008, **10**, 1555-1558.
- (a) M. P. de Jong, L. van IJzendoorn and M. J. A. de Voigt, *Appl. Phys. Lett.*, 2000, **77**, 2255-2257. (b) Y. J. Lee, *Synth. Met.*, 2006, **156**, 537-540. (c) K. W. Wong, H. L. Yip, Y. Luo, K. Y. Wong, W. M. Lau, K. H. Low, H. F. Chow, Z. Q. Gao, W. L. Yeung and C. C. Chang, *Appl. Phys. Lett.*, 2002, **80**, 2788-2790.
- (a) L. S. C. Pingree, B. A. Macleod and D. S. Ginger, *J. Phys. Chem. C*, 2008, **112**, 7922-7927. (b) S. K. M. J nsson, J. Birgeron, X. Crispin, G. Greczynski, W. Osikowicz, A. W. Denier van der Gon, W. R. Salaneck and M. Fahlman, *Synth. Met.*, 2003, **139**, 1-10.
- M. Kemerink, S. Timpanaro, M. M. d. Kok, E. A. Meulenkaamp and F. J. Touwslager, *J. Phys. Chem. B*, 2004, **108**, 18820-18825.
- (a) P. Peumans and S. R. Forrest, *Appl. Phys. Lett.*, 2001, **79**, 126-128. (b) H. Yan, P. Lee, N. R. Armstrong, A. Graham, G. A. Evmenenko, P. Dutta and T. J. Marks, *J. Am. Chem. Soc.*, 2004, **127**, 3172-3183.
- (a) F. Huang, Y.-J. Cheng, Y. Zhang, M. S. Liu and A. K. Y. Jen, *J. Mater. Chem.*, 2008, **18**, 4495-4509. (b) A. C. Morteani, A. S. Dhoot, J.-S. Kim, C. Silva, N. C. Greenham, C. Murphy, E. Moons, S. Cina and J. H. Burroughes, *Adv. Mater.*, 2003, **15**, 1708-1712. (c) A. C. Morteani, P. K. H. Ho, R. H. Friend and C. Silva, *Appl. Phys. Lett.*, 2005, **86**, 162501. (d) Q. J. Sun, B. H. Fan, Z. A. Tan, C. H. Yang, Y. F. Li and Y. Yang, *Appl. Phys. Lett.*, 2006, **88**, 163510. (e) R. J. Holmes, B. W. D'Andrade, S. R. Forrest, X. Ren, J. Li and W. E. Thompson, *Appl. Phys. Lett.*, 2003, **83**, 3818. (f) J. Feng, F. Li, W. Gao, S. Liu, Y. Liu and Y. Wang, *Appl. Phys. Lett.*, 2001, **78**, 3947. (g) N. Matsumoto, M. Nishiyama and C. Adachi, *J. Phys. Chem. C*, 2008, **112**, 7735-7741. (h) D. D. Gebler, Y. Z. Wang, J. W. Blatchford, S. W. Jessen, D.-K. Fu, T. M. Swager, A. G. MacDiarmid and A. J. Epstein, *Appl. Phys. Lett.*, 2001, **70**, 1644. (i) X. Jiang, M. S. Liu and A. K. Y. Jen, *J. Appl. Phys.*, 2002, **91**, 10147-10152. (j) J. Morgado, R. H. Friend and F. Cacialli, *Appl. Phys. Lett.* 2002, **80**, 2436. (k) H. Yan, B. J. Scott, Q. Huang and T. J. Marks, *Adv. Mater.* 2004, **16**, 1948-1953. (l) Tang, C. W.; VanSlyke, S. A. *Appl. Phys. Lett.* **1987**, *51*, 913.
- (a) E. Bellmann, S. E. Shaheen, R. H. Grubbs, S. R. Marder, B. Kippelen and N. Peyghambarian, *Chem. Mater.*, 1990, **11**, 399-407. (b) S. E. Shaheen, G. E. Jabbour, B. Kippelen, N. Peyghambarian, J. D. Anderson, S. R. Marder, N. R. Armstrong, E. Bellmann and R. H. Grubbs, *Appl. Phys. Lett.*, 1999, **74**, 3212. (c) Y. Shirota, *J. Mater. Chem.* **2000**, *10*, 1-25.
- (a) P. K. H. Ho, J.-S. Kim, J. H. Burroughes, H. Becker, S. F. Y. Li, T. M. Brown, F. Cacialli and R. H. Friend, *Nature*, 2000, **404**, 481-484. (b) Q. Huang, G. A. Evmenenko, P. Dutta, P. Lee, N. R. Armstrong and T. J. Marks, *Acc. Chem. Res.*, 2005, **127**, 10227-10242. (c) J. G. C. Veinot and T. J. Marks, *Acc. Chem. Res.*, 2005, **38**, 632-643. (d) Y. Lim, Y. S. Park, Y. Kang, Y. Jang do, J. H. Kim, J. J. Kim, A. Sellinger and Y. Yoon do, *J. Am. Chem. Soc.*, 2011, **133**, 1375-1382.

- 12 (a) X. Gong, S. Wang, D. Moses, G. C. Bazan and A. J. Heeger, *Adv. Mater.*, 2005, **17**, 2053-2058. (b) W. Ma, P. K. Iyer, X. Gong, B. Liu, D. Moses, G. C. Bazan and A. J. Heeger, *Adv. Mater.*, 2005, **17**, 274-277. (c) F. Huang, L. Hou, H. Wu, X. Wang, H. Shen, W. Cao, W. Yang and Y. Cao, *J. Am. Chem. Soc.*, 2004, **126**, 9845-9853. (d) H. Wu, F. Huang, Y. Mo, W. Yang, D. Wang, J. Peng and Y. Cao, *Adv. Mater.*, 2004, **16**, 1826-1830.
- 13 (a) J. Zhao, J. A. Bardecker, A. M. Munro, M. S. Liu, Y. Niu, I.-K. Ding, J. Luo, B. Chen, A. K.-Y. Jen and D. S. Ginger, *Nano Lett.*, 2006, **6**, 463-467. (b) S. Liu, X. Jiang, H. Ma, M. S. Liu and A. K.-Y. Jen, *Macromolecules*, 2000, **33**, 3514-3517. (c) G. K. Paul, J. Mwaura, A. A. Argun, P. Taraneekar and J. R. Reynolds, *Macromolecules*, 2006, **39**, 7789-7792.
- 14 Y.-J. Cheng, M.-H. Liao, H.-M. Shih, P.-I. Shih and C.-S. Hsu, *Macromolecules*, 2011, **44**, 5968-5976.
- 15 (a) K. S. Khuong, W. H. Jones, W. A. Pryor and K. N. Houk, *J. Am. Chem. Soc.*, 2005, **127**, 1265-1277. (b) F. Mayo, *J. Am. Chem. Soc.*, 1968, **90**, 1289-1295. (c) Y. K. Chong, E. Rizzardo and D. H. Solomon, *J. Am. Chem. Soc.*, 1983, **105**, 7761-7762.
- 16 Y.-J. Cheng, M. S. Liu, Y. Zhang, Y. Niu, F. Huang, J.-W. Ka, H.-L. Yip, Y. Tian and A. K.-Y. Jen, *Chem. Mater.*, 2008, **20**, 413-422.
- 17 (a) K. Walzer, B. Maennig, M. Pfeiffer and K. Leo, *Chem. Rev.*, 2007, **107**, 1233-1271. (b) T. Matsushima and C. Adachi, *Appl. Phys. Lett.*, 2006, **89**, 253506. (c) T. Oyamada, H. Sasabe, C. Adachi, S. Murase, T. Tominaga and C. Maeda, *Appl. Phys. Lett.*, 2005, **86**, 033503. (d) M. Pfeiffer, A. Beyer, T. Fritz and K. Leo, *Appl. Phys. Lett.*, 1998, **73**, 3202. (e) T. Matsushima and C. Adachi, *J. Appl. Phys.*, 2008, **103**, 034501. (g) Y. Qi, T. Sajoto, S. Barlow, E.-G. Kim, J.-L. Brédas, S. R. Marder and A. Khan, *J. Am. Chem. Soc.*, 2009, **131**, 12530-12531.
- 18 Y. Sun, S.-C. Chien, H.-L. Yip, Y. Zhang, K.-S. Chen, D. F. Zeigler, F.-C. Chen, B. Lin and A. K. Y. Jen, *Chem. Mater.*, 2011, **23**, 5006-5015.
- 19 (a) B. Olofsson and E. A. Merritt, *Angew. Chem. Int. Ed.*, 2009, **48**, 9052-9070. (b) H. Gu, K. Ren, O. Grinevich, J. H. Malpert and D. C. Neckers, *J. Org. Chem.*, 2001, **66**, 4161-4164.
- 20 (a) A. B. Tamayo, B. Walker and T.-Q. Nguyen, *J. Phys. Chem. C*, 2008, **112**, 11545-11551. (b) B. Walker, A. B. Tomayo, X. D. Dang, P. Zalar, J. H. Seo, A. Garcia, M. Tantiwiwat and T.-Q. Nguyen, *Adv. Funct. Mater.*, 2009, **19**, 3063-3069.
- 21 (a) J. H. Seo, A. Gutacker, Y. Sun, H. Wu, F. Huang, Y. Cao, U. Scherf, A. J. Heeger and G. C. Bazan, *J. Am. Chem. Soc.*, 2011, **133**, 8416-8419. (b) H.-Y. Chen, J.-H. Hou, S. Zhang, Y. Liang, G. Yang, Y. Yang, L. Yu, Y. Wu and G. Li, *Nat. Photon.*, 2009, **3**, 649-653.
- 22 (a) Y. Liang, Z. Xu, J. Xia, S.-T. Tsai, Y. Wu, G. Li, C. Ray and L. Yu, *Adv. Mater.*, 2010, **22**, E135-E138. (b) S. J. Lou, J. M. Szarko, T. Xu, L. Yu, T. J. Marks and L. X. Chen, *J. Am. Chem. Soc.*, 2011, **133**, 20661-20663. (c) J. You, C.-C. Chen, L. Dou, S. Murase, H.-S. Duan, S. A. Hawks, T. Xu, H. J. Son, L. Yu, G. Li and Y. Yang, *Adv. Mater.*, 2012, **24**, 5267-5272. (d) L. Lu and L. Yu, *Adv. Mater.*, 2014, **26**, 4413-4430. (e) M. Zhang, Y. Gu, X. Guo, F. Liu, S. Zhang, L. Huo, T. P. Russell and J. Hou, *Adv. Mater.*, 2013, **25**, 4944-4949.
- 23 Y.-L. Chen, W.-S. Kao, C.-E. Tsai, Y.-Y. Lai, Y.-J. Cheng and C.-S. Hsu, *Chem. Commun.*, 2013, **49**, 7702-7704.
- 24 (a) G. Zhou, Y. He and Y. Li, *J. Am. Chem. Soc.*, 2010, **22**, 4355-4358. (b) C.-H. Hsieh, Y.-J. Cheng, P.-J. Li, C.-H. Chen, M. Dubosc, R.-M. Liang and C.-S. Hsu, *J. Am. Chem. Soc.*, 2010, **132**, 4887-4893. (c) C.-Y. Chang, C.-E. Wu, S.-Y. Chen, C. Cui, Y.-J. Cheng, C.-S. Hsu, Y.-L. Wang and Y. Li, *Angew. Chem. Int. Ed.*, 2011, **50**, 9386-9390. (d) Y.-Y. Lai, Y.-J. Cheng and C.-S. Hsu, *Energy Environ. Sci.*, 2014, **7**, 1866-1883.

